ROYAL SOCIETY
OF CHEMISTRY

PAPER

Low-temperature heat capacity and the thermodynamic functions of a novel ether-based ionic liquid 1-(2-ethoxyethyl)-3-ethylimidazolium thiocyanate†

Donglu Fu,[a] Zongren Song, [iD] *[a] Jiankang Liu,[a] Jie Yang,[a] Shilong Suo,[a] Kunhao Liang,*[b] Xiaoxue Ma*[a] and Dawei Fang [iD] [a]

A novel ionic liquid (IL) modified by ether was prepared by a two-step synthesis method for the first time in this paper. The structure of 1-(2-ethoxyethyl)-3-ethylimidazolium thiocyanate ([C₂O2Im][SCN]) was characterized and analyzed by hydrogen nuclear magnetic resonance (¹H-NMR), carbon nuclear magnetic resonance (¹³C-NMR), Fourier transform infrared spectroscopy (FT-IR), electrospray ionization-mass spectrometry (ESI-MS), elemental analysis and thermal gravity analysis (TG). Within a specific temperature range from 79 to 393 K, the low temperature heat capacity of [C₂O2Im][SCN] was determined, using a high precision low temperature adiabatic calorimeter. Then, the related thermodynamic functions, such as $(H_T - H_{298.15})$, $(S_T - S_{298.15})$ and $(G_T - G_{298.15})$, were calculated, which can provide a theoretical basis for the application of ether-based ILs in the future.

1. Introduction

Ionic liquids (ILs) are regarded as designer solvents consisting of organic cations and organic or inorganic anions, which constitute innovative fluids for chemical processes. ILs can be used as substitutes for volatile solvents and heat transfer fluids. They are considered as good candidates for replacements of volatile solvents and heat transfer liquids, due to the excellent properties of non-flammability and negligible vapor pressure under normal environmental conditions.[1,2] Heat transfer fluids with high heat capacity and low viscosity are used most widely. A new type of heat transfer media, so-called ionanofluids (INFs), has been intensively studied in recent years. This is a group of nanodispersions in which ionic liquids (ILs) form the continuous phase.[3] The most promising thermophysical properties are from cyano alkylimidazolium-based INFs due to the relatively high thermal conductivity and low viscosity of their base liquids compared to other known ILs.[4,5] The thermophysical parameters of ILs are quite similar to those of widely used organic and organo-silicon heat transfer fluids.[6] An important feature that distinguishes ILs among other heat transfer fluids is the exceptionally low saturated vapour pressure at high temperature. This makes them non-volatile and non-explosive and especially attractive for operation under dynamic vacuum and perhaps in outer space. The ionic liquid introduces an ether group and cyano group to make it have better performance.[7–13] Additionally, the high electronegativity and stable triple bond of cyano-based ILs offered them high conductivity and high fluidity.[14]

Heat capacity as a sensitive indicator of phase transitions is not only one of the most important thermophysical properties of matter, but also one of the basic thermodynamic properties of liquid.[15,16] On the basis of heat capacity, the temperature-dependent thermodynamic properties such as entropy, enthalpy and Gibbs energy can be derived. Moreover, the heat capacities are a necessary parameter to evaluate the effect of temperature on phase equilibrium and reaction equilibrium. The heat capacities and thermal transitions of ILs are important parameters for the selection of operating temperature range in industrial processes.[17]

The properties of ionic liquids can be regulated by changing the anions and cations of ILs, and the prediction method is widely used in the study of ILs properties, including the ILs heat capacity. Recently, the group contribution method (GCM),[18] quantitative structure property relationship (QSPR),[19] group-additivity method (GAM),[20] group method of data handling (GMDH),[21] artificial neural network (ANN),[22] multiple linear regression (MLR) and extreme learning machine (ELM) methods,[23] *etc.* have been widely applied to estimate the ILs heat capacity. Although the prediction accuracy is acceptable, the cations and anions introduced in the derivation of the model are not comprehensive enough which confines the prediction

[a]Institute of Rare and Scattered Elements, College of Chemistry, Liaoning University, Shenyang, Liaoning 110036, China. E-mail: zongrensong@lnu.edu.cn

[b]School of Opto-Electronic Engineering, Zaozhuang University, Zaozhuang, Shandong 277160, China

capability of the proposed model. At present, the main methods for determination of the ILs heat capacity have been reported, including high-precision heat capacity drop calorimetry,[24] differential scanning calorimetry,[25,26] isothermal titration calorimetric[27] and adiabatic calorimetry.[28] Currently, the high reliability of the data measured by low temperature adiabatic calorimeter is attributed to its highly intelligent modern control theory calorimetric system.[29]

In our case, the low temperature heat capacity of ILs has been measured by high precision automated adiabatic calorimeter.[30,31] However, with the continuous development of ILs, the data of the basic properties is still lacking. Based on the improvement of the structure of the ionic liquids synthesized in the previous work, a new ether-functionalized IL – 1-(2-ethoxyethyl)-3-ethylimidazole thiocyanate ([C$_2$O2Im][SCN]) was prepared for the first time. The ionic liquid introduces ether group and thiocyanate group to make it have better performance. The growth of the alkyl chain on the cationic ethoxy group is expected to further reduce the viscosity of the ionic liquids studied in this paper. The alkoxyethyl (2OR) group was favorable to decrease viscosity, and the high electronegativity and stable triple bond of thiocyanate ILs offered them high conductivity and high fluidity.[10–12,32] The data of low temperature heat capacity of [C$_2$O2Im][SCN] was obtained by the low temperature adiabatic calorimeter at the temperature between 79 K and 393 K. According to the values of experiment heat capacity, the related thermodynamic functions in the temperature range from (300 to 390 K) $\pm$ 5 K, such as $H_T - H_{298.15}$, $S_T - S_{298.15}$ and $G_T - G_{298.15}$ of [C$_2$O2Im][SCN] were obtained. Ionic liquids are considered to be promising candidates for heat transfer liquid. The above experimental results can provide the operating temperature range for the novel IL [C$_2$O2Im][SCN] as a heat transfer liquid in the industrial applications.

2. Experimental

2.1 Reagents

The purities and sources of the reagents are listed in Table 1.

2.2 Preparation and characterization of [C$_2$O2Im][SCN]

The IL [C$_2$O2Im][SCN] was synthesized by the Fig. 1. Firstly, 1.1 mol of 2-chloroethyl ethyl ether was added dropwise into the flask containing the 1 mol of 1-ethylimidazole stirring at 75 °C for 48 h, then the 1-(2-ethoxyethyl)-3-ethylimidazolium chloride [C$_2$O2Im][Cl] as precursor was obtained.[33,34] Secondly,
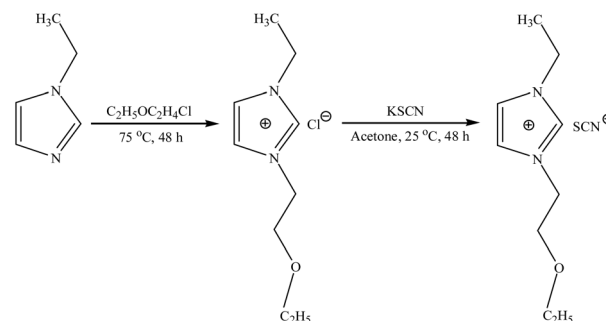

Fig. 1 Synthesis of the novel ether-functionalized IL [C$_2$O2Im][SCN].

dissolving 1 mol of the [C$_2$O2Im][Cl] in a beaker containing about twice the volume of acetone, and then adding 1.2 mol of potassium thiocyanate in the beaker at 25 °C for 48 h. The product was purified by filtration with filter paper that is excess potassium thiocyanate was removed, and then the filtrate was collected and steamed to remove excess acetone at 56 °C. Finally, the target product was dried *in vacuo* (10^{-2} mbar) for 24 h at 70 °C, vacuum environment was obtained using rotary vane vacuum pump, and the target IL was obtained.

Subsequently, the [C$_2$O2Im][SCN] were characterized by ^{1}H-NMR spectroscopy (Mercury-Vx300, Varian, USA), ^{13}C-NMR spectroscopy (Mercury-Vx300, Varian, USA), FT-IR spectroscopy (IR Perstige, Shimadzu Corporati, Japan), electrospray ionization mass spectrometry (ESI-MS, Thermo Scientific Q Exactive), element analysis (PerkinElmer 2400) and thermogravimetry (TG, SDT Q600) (see Fig. S1–S5 in the ESI material†). Then the mass fraction of water content ($w\%$) was determined by a Karl Fischer moisture titrator (ZSD – 2 type) and $w\%$ < 0.003. ^{1}H-NMR (DMSO-d$_6$): δ_H = 9.15 (s, 1H), 7.81 (s, 1H), 7.74 (s, 1H), 4.33 (t, 2H), 4.21 (m, 2H), 3.72 (t, 2H), 3.46 (m, 2H), 1.42 (t, 3H), 1.07 (t, 3H). ^{13}C-NMR (DMSO-d$_6$): 126.07, 121.81, 117.54, 113.28, 65.17, 61.87, 61.03, 58.16, 20.65, 19.43. The IR spectrum of [C$_2$O2Im][SCN] exhibited the characteristic absorption of the thiocyanate functionality at 2060 cm^{-1}, and ether group functionality at 1108 cm^{-1}. The ESI-MS Figure shows that MS$^+$ m/z: 169.1 [C$_2$O2Im]$^+$, MS$^-$ m/z: 58.0 [SCN]$^-$. Anal. Calcd for C$_{10}$H$_{17}$N$_3$OS: C, 52.77; H, 7.68; N, 18.41. The TG curve shows that the initial decomposition temperature of [C$_2$O2Im][SCN] is 270.72 °C, which corresponds to the peak value of the DTG curve, that is, the temperature at which the mass change rate is the largest. Herein, the sample purity of [C$_2$O2Im][SCN] was more than 99%.

Table 1   The purities and sources of the reagents

Reagent	CAS	Purity	Source
1-Ethylimidazole	7098-07-9	>98%	Adamas
2-Chloroethyl ethyl ether	628-34-2	>98%	Adamas
Ethyl acetate	141-78-6	>99.5%	Sinopharm Chemical Reagent Co., Ltd
Acetone	67-64-1	>99.5%	Sinopharm Chemical Reagent Co., Ltd
Potassium thiocyanate	333-20-0	≥98.5%	Greagent
α-Al$_2$O$_3$(s)		>99.95%	National Institute of Standards and Technology
Ultrapure water			Prepared by multiple distillation

2.3 Measurement of molar heat capacities of [C$_2$2O2Im][SCN] by adiabatic calorimeter

Before the measurement, IL sample was dried *in vacuo* (10^{-2} mbar) for 24 h at 80 °C, and the sample pool and the insulation screen were thoroughly cleaned with anhydrous ethanol, and the sample pool was sealed with an organic thermal conductive silicone ring after drying. Helium was filled to ensure that the sample pool was uniformly heated during the experiment. After the colloid was cured, make sure the tightness of the sample cell was good, insert the platinum resistance thermometer and the inner screen thermocouple at the bottom of the sample cell, assemble and seal them, and vacuum until the pressure gauge shows 10^{-2}–10^{-3} mbar. Make sure the connection of the line was correct, and the room temperature condition begins the pre-test. When the temperature of the system was reduced to about 78 K and vacuumed, the experiment was carried out in the temperature range of 78–400 K with 3 K as the interval.

In this work, the heat capacity was measured by the high precision automatic adiabatic calorimeter, which developed by Dalian Institute of Chemical Physics.[35,36] The accuracy of the instrument measurement is ±0.001 K for temperature. Herein, we chose the α-Al$_2$O$_3$ as a reference standard material to verify the reliability of the adiabatic calorimeter, and then the data of heat capacity of empty equivalent and the α-Al$_2$O$_3$ were obtained at 3 K intervals at temperatures ranging from 78.254 to 400.134 K and 79.432 to 400.854 K, respectively. And then, the corresponding experimental values of the data are listed in Tables S1 and S2,† and described in the Fig. 2. From Table S1,† it can be seen that two peaks at 223.480 K and 226.649 K, which were caused by the melting of organic heat transfer silica gel and silicone, implying that they didn't affect existing calibration. Furthermore, the heat capacity experimental data of empty equivalent and the α-Al$_2$O$_3$ were fitted by the least square method, and adopted polynomial segmentation fitting to match experimental data.[37] The fitted values and corresponding relative deviation are also listed in Tables S3 and S4.† From the comparison, we know that the deviations between experimental values and the fitting values are within ±0.5% in the

temperature range of 78 to 400 K. Additionally, the deviations between heat capacity fitted values of α-Al$_2$O$_3$ and the recommended values by NIST[38,39] are within ±0.5% (see Table S5†), and the uncertainty compared with the values given by the former National Bureau of Standards[37] are within ±0.159%. After that, the molar heat capacities of [C$_2$2O2Im][SCN] (1.15172 g) were repeatedly measured by calibrated adiabatic calorimeter at 3 K intervals at temperatures ranging from 78 to 400 K.

In this experimental, the sealing was carried out twice. Firstly, the organic silica gel was used to seal the experimental sample in the sample pool (Fig. S6I†). When sealing this time, the sample pool was filled with helium gas. Secondly, the assembled sample pool (Fig. S6I†) and the internal and external insulation screen (Fig. S6H and G†) were sealed in a steel vacuum tank (Fig. S6L†) using flanges and lead pads (Fig. S6D†). During sealing this time, the vacuum tank was vacuumed. The assembly of the two seals and the insulating screen was conducive to creating an insulating environment, which can improve the accuracy of the experimental results. Herein, the details of calorimeter can be referred to the Fig. S6.†

3. Results and discussion

3.1 Heat capacity

Firstly, we consider the factors affecting the uncertainty before determining the molar heat capacity. These factors include the standard uncertainty of maximum error of the instrument, multiple measurements, mass of sample experiment, sample purity,[40] which are denoted as $u(\text{MPE})$, $u(\text{sd})$, $u(\text{Mass})$ and $u(\text{Purity})$, respectively. And then, the expanded uncertainties (0.95 confidence level, $k \approx 2$), U, of each measured variable are obtain and show in Table 2 and S6,† respectively.

The first set of experimental molar heat capacities of [C$_2$2O2Im][SCN] in the temperature range 79.314 to 392.911 K with 3 K intervals are showed in Table 2 and Fig. 3. Another set of experimental data in the corresponding temperature range are listed in Table S6 and Fig. S7,† respectively.

The heat capacity curve in Fig. 3 was shown the smooth upward trend in the temperature ranges of 79.314–178.027 K, 191.547–224.826 K, 266.528–392.911 K, which implied that the [C$_2$2O2Im][SCN] was presented glass state, solid state and liquid state in the corresponding temperature range, respectively. The curve was also indicated that the IL has a wide liquid temperature range and was stable in liquid state. Besides, the heat capacity curve was raised significantly in the temperature range of 181.011–188.585 K and 230.801–263.644 K, one was accompanied by the glass transition process of [C$_2$2O2Im][SCN], and the other one was along with the melting process with the phase transition from solid to liquid. The glass transition temperature (T_g) and the melting point (T_m) were obtained by the two sets of experimental molar heat capacities of [C$_2$2O2Im][SCN], which were (184.383 ± 0.417) K and (256.606 ± 0.033) K, respectively. Fig. 4 contains two series of heat capacity, which measured in the fusion region. It indicates that the fusion process of [C$_2$2O2Im][SCN] is reversible and repeatable. The experimental results further prove that the low temperature adiabatic calorimeter has good accuracy and repeatability. Herein, the molar
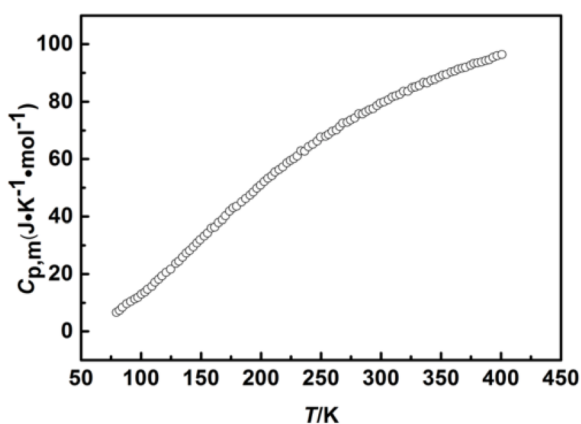

Fig. 2 The heat capacities of α-Al$_2$O$_3$ in the temperature range from 78 to 400 K.

Table 2 The first set of experimental values of molar heat capacity for [C$_2$2O2Im][SCN] in the temperature range from 79.314 to 392.911 K with 3 K intervals[a]

T/(K)	$C_{p,m}$ (J K^{-1} mol^{-1})	T/(K)	$C_{p,m}$ (J K^{-1} mol^{-1})	T/(K)	$C_{p,m}$ (J K^{-1} mol^{-1})
79.314	85.777	184.800	206.123	295.680	327.854
81.371	90.607	188.585	266.752	298.580	328.438
84.331	94.426	191.547	269.519	301.433	330.697
87.201	96.424	194.499	267.017	304.284	330.725
90.065	97.935	197.516	270.874	307.135	330.924
92.933	100.078	200.597	273.125	310.009	331.504
95.806	100.968	203.666	274.209	313.002	331.953
98.685	102.111	206.720	275.433	316.185	332.599
101.582	103.296	209.741	273.398	319.227	333.018
104.491	104.476	212.724	277.361	322.299	334.604
107.417	107.291	215.733	277.824	325.380	335.706
110.362	108.836	218.771	278.526	328.272	336.430
113.297	109.582	221.789	279.494	331.149	337.220
116.222	110.499	224.826	280.574	334.019	337.811
119.172	111.608	227.862	286.044	336.885	339.305
123.230	114.551	230.801	289.408	339.751	340.362
127.267	117.278	233.806	325.825	342.616	340.854
130.226	118.990	236.918	396.433	345.485	340.687
133.207	121.442	239.930	467.398	348.353	341.968
136.161	123.619	243.560	589.361	351.228	343.444
139.141	125.223	247.524	976.824	354.116	344.806
142.148	127.087	252.560	1878.526	357.017	347.168
145.129	129.108	256.638	3282.494	359.933	347.383
148.091	130.410	260.735	890.574	362.885	348.691
151.081	132.506	263.644	398.044	365.847	352.645
154.102	134.291	266.528	318.408	368.815	354.508
157.103	135.796	269.494	319.825	371.796	356.890
160.088	137.301	272.465	322.045	374.787	360.192
163.057	138.191	275.417	322.839	377.791	360.270
166.011	139.216	278.328	323.783	380.792	363.985
168.999	139.851	281.218	324.577	383.812	369.880
172.023	141.183	284.086	324.898	386.839	374.305
175.030	141.607	286.928	326.313	389.872	376.220
178.027	142.572	289.826	325.780	392.911	379.381
181.011	153.204	292.789	327.025		

[a] T is Kelvin temperature, and $C_{p,m}$ is molar heat capacities. The standard uncertainty (0.68 level of confidence): $u(T) = 0.001$ K, $u(p) = 0.001$ MPa. The expanded uncertainties $U(C_{p,m})$ is at 0.95 confidence level, ($k \approx 2$), $U_c(C_{p,m}) = 0.002 \cdot C_{p,m}$.
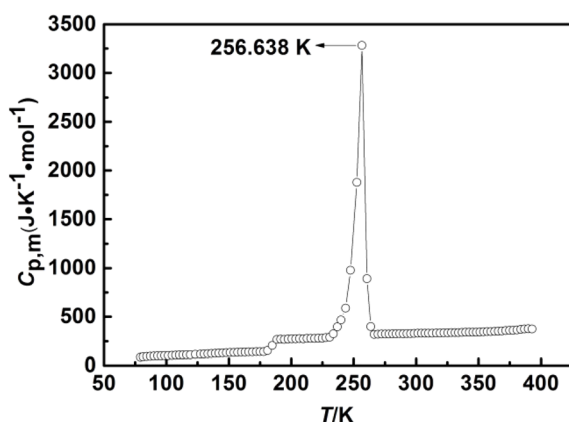
Fig. 3 The experimental molar heat capacities in Table 2 of [C$_2$2O2IM][SCN] in the temperature range from 79 to 393 K.
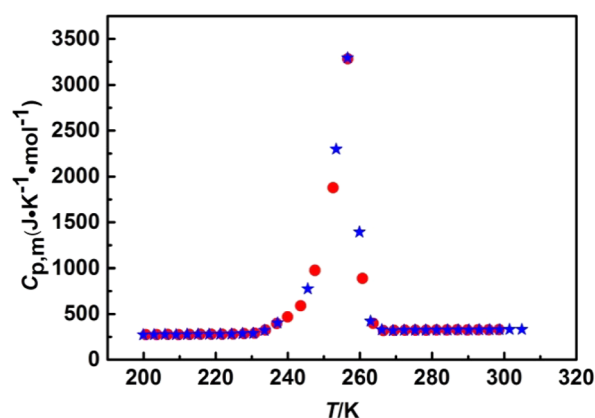

Fig. 4 Two series of experimental molar heat capacities of [C$_2$2O2IM][SCN] in the fusion region (● red solid circle is the first series, ★ blue solid pentacle is the second series).

heat capacities of [C$_2$2O2Im][SCN] in Table 2 are fitted by piecewise polynomial in reduced temperature (x), using the least square method in the certain temperature range.[30,31,41]

The fitting equation for the first temperature range of 79–178 K is following:

$$x = (T - 128.5)/49.5 \qquad (1)$$

$$C_{p,m}/(\text{J K}^{-1} \text{ mol}^{-1}) = 118.17577 + 32.78655x + 4.93784x^2 - 18.93691x^3 - 1.641x^4 + 14.251x^5 - 7.22955x^6 \qquad (2)$$

For the second temperature range 192–225 K:

$$x = (T - 208.5)/16.5 \qquad (3)$$

$$C_{p,m}/(\text{J K}^{-1} \text{ mol}^{-1}) = 275.99163 + 4.96005x - 1.31058x^2 + 1.17008x^3 - 2.12929x^4 - 0.52521x^5 + 2.55262x^6 \qquad (4)$$

For the third temperature range 267–346 K:

$$x = (T - 306.5)/39.5 \qquad (5)$$

$$C_{p,m}/(\text{J K}^{-1} \text{ mol}^{-1}) = 331.03056 + 6.62813x - 0.79168x^2 + 10.22054x^3 + 5.34842x^4 - 5.90238x^5 - 5.89985x^6 \qquad (6)$$

For the finally temperature range 347–393 K:

$$x = (T - 370)/23 \qquad (7)$$

$$C_{p,m}/(\text{J K}^{-1} \text{ mol}^{-1}) = 355.3121 + 17.58326x - 0.86388x^2 + 6.26081x^3 + 24.72321x^4 - 4.42713x^5 - 19.54869x^6 \qquad (8)$$

The correlation coefficient of the fitting $R^2 = 0.99905$, $R^2 = 0.99702$, $R^2 = 0.99685$ and $R^2 = 0.99204$, respectively. In the

Table 4 Results of phase transition of the [C$_2$2O2Im][SCN] obtained from both series of heat capacity measurements[a]

	[C$_2$2O2Im][SCN]		
Thermodynamic functions	Series 1, x_1	Series 2, x_2	$\bar{x} \pm \sigma_a$
T_g/(K)	184.800	183.966	184.398 ± 0.566
T_m/(K)	256.638	256.573	256.606 ± 0.046
$\Delta_{fus}H_m$/(kJ mol^{-1})	19.724	18.688	19.206 ± 0.518
$\Delta_{fus}S_m$/(J K^{-1} mol^{-1})	76.855	72.837	74.846 ± 2.009

[a] $\sigma_a = [\sum_{i=1}^{n}(x_i - \bar{x})^2/n(n-1)]^{1/2}$ in which n is the experimental number; x_i, a single value in a set of calorimetric measurements; $\bar{x}$, the mean value of a set of measurement results.

fitting temperature region, $x = [T - (T_{max} + T_{min})/2]/[(T_{max} - T_{min})/2]$, T is the thermodynamic temperature of experiment.

3.2 Thermodynamic functions

The related thermodynamic functions with 298.15 K as reference temperature, such as $(H_T - H_{298.15})$, $(S_T - S_{298.15})$ and $(G_T - G_{298.15})$, were calculated by the polynomial equation of heat capacity in the temperature range from 300 to 390 K with 5 K intervals, and the thermodynamic relationships as follows:

$$H_T - H_{298.15} = \int_{298.15}^{T} C_{p,m} \, dT \qquad (9)$$

$$S_T - S_{298.15} = \int_{298.15}^{T} (C_{p,m}/T) \, dT \qquad (10)$$

$$G_T - G_{298.15} = \int_{298.15}^{T} C_{p,m} \, dT - \mathsf{T}\int_{298.15}^{\mathsf{T}} (C_{p,m}/T) \, dT \qquad (11)$$

Table 3 The calculated values of thermodynamic functions data for [C$_2$2O2Im][SCN] in[a] the temperature range from (300–390) K

T/(K)	$C_{p,m}$/(J K^{-1} mol^{-1})	$H_T - H_{298.15}$/(kJ mol^{-1})	$S_T - S_{298.15}$/(J K^{-1} mol^{-1})	$-(G_T - G_{298.15})$/(kJ mol^{-1})
298.15	329.5	—	—	—
300	329.9	0.60	2.04	0.012
305	330.8	2.26	7.51	0.031
310	331.6	3.92	12.9	0.079
315	332.5	5.58	18.2	0.153
320	333.6	7.25	23.4	0.238
325	335.1	8.92	28.6	0.375
330	336.8	10.6	33.7	0.521
335	338.7	12.3	38.8	0.698
340	340.3	14.0	43.8	0.892
345	340.8	15.7	48.7	1.102
350	343.1	17.4	53.6	1.360
355	345.2	19.1	58.5	1.668
360	347.8	20.9	63.4	1.924
365	351.4	22.6	68.2	2.293
370	355.3	24.4	73.0	2.610
375	359.2	26.2	77.8	2.975
380	364.0	28.0	82.6	3.388
385	370.6	29.8	87.4	3.849
390	377.5	31.7	92.2	4.425

[a] T is Kelvin temperature, and $C_{p,m}$ is molar heat capacities.

The thermodynamic functions $(H_T - H_{298.15})$, $(S_T - S_{298.15})$ and $-(G_T - G_{298.15})$ were calculated and the values are listed in Table 3, and the changing trend of these data is the same as that reported in the literature.[25,26] Then, plotting the values of $H_T - H_{298}$ vs. T, and the fitted line is shown in Fig. S8.† In the temperature range of 300 to 390 K, the values of $(H_T - H_{298})$ increase with the increasing temperatures. $(H_T - H_{298.15})$, $(S_T - S_{298.15})$ and $-(G_T - G_{298.15})$ are positively correlated with temperature. Compared with the ionic liquid 1-(2-methoxyethyl)-3-ethylimidazolium perrhenate $[C_2O1IM][ReO_4]$ in literature 31, the values of $C_{p,m}$, $(H_T - H_{298.15})$, $(S_T - S_{298.15})$ and $-(G_T - G_{298.15})$ are less than those in this study.

The molar enthalpy $\Delta_{fus}H_m$ and entropy $\Delta_{fus}S_m$ of fusion of the compound are obtained by the following equations:

$$\Delta_{fus}H_m = \left(Q - n\int_{T_i}^{T_f} C_{p,m(S)}dT - n\int_{T_i}^{T_f} C_{p,m(L)}dT - \int_{T_i}^{T_f} C_0 dT \right) \Big/ n \tag{12}$$

$$\Delta_{fus}S_m = \Delta_{fus}H_m / T_m \tag{13}$$

where T_i and T_f are the temperature at the initial or final melting temperature, Q is the total energy introduced to the sample cell from T_i to T_f, $C_{p(S)}$ and $C_{p(L)}$ are the heat capacity of the sample in the solid phase and liquid phase at T_i and T_f, respectively. $C_{p(L)}$ is the heat capacity of the sample in liquid phase at C_0 is the average heat capacity of the empty sample cell at temperature $(T_i + T_f)/2$. The results of the melting point (T_m), molar enthalpy $(\Delta_{fus}H_m)$, and molar entropy $(\Delta_{fus}S_m)$ of two phases transition obtained from every series of repeated experiments are listed in Table 4.

From Table 4, the average value of T_m is 256.606 ± 0.046 K for the two series of repeated experiments, which is higher than T_g. The IL $[C_2O2Im][SCN]$ changes from a glassy state to a highly elastic state and then from a solid state to a liquid state during this temperature change (211.826 K),[26] it may be due to the effect of the size of the anionic group on steric hindrance. When the cation structure of IL is the same, the volume of anion directly affects its steric resistance, that is, the volume of anion is proportional to its steric resistance, and inversely proportional to the melting temperature. This result is similar to the literature reports.[42,43] Due to the similar thermal stability of most kinds of ILs, the melting temperatures are relatively close, resulting in the values of melting enthalpy and melting entropy are relatively close.[31,42,43]

4. Conclusions

Heat capacity as a key reference for phase transition of matter is not only one of the most important thermophysical properties of matter, but also one of the basic thermodynamic properties of liquid. Herein, the heat capacities of the novel ether-functionalized IL $[C_2O2Im][SCN]$ were obtained by the calibrated high precision low temperature adiabatic calorimeter at the temperatures between 79 K and 393 K. The glass state, solid state and liquid state temperature ranges of $[C_2O2Im][SCN]$

were obtained by the heat capacity curve, that is 79–178 K, 192–225 K and 267–393 K, respectively. In the meantime, the glass transition temperature $(T_g = 184.383 \pm 0.417$ K$)$ and the melting point $(T_m = 256.606 \pm 0.033$ K$)$ were also obtained. Finally, the related thermodynamic functions $(H_T - H_{298.15})$, $(S_T - S_{298.15})$ and $(G_T - G_{298.15})$ were obtained by polynomial equation of heat capacity values in the temperature range from 300 to 390 K with 5 K intervals. The above experimental results can provide the operating temperature range for the novel IL $[C_2O2Im][SCN]$ as a heat transfer liquid in the industrial applications.

Data availability

The data supporting this article have been included as part of the ESI.†

Conflicts of interest

There are no conflicts to declare.

Acknowledgements

Notes and references

1 D. K. Verma, Y. Dewangan, A. K. Singh, R. Mishra, M. A. Susan, R. Salim, M. E. Taleb, F. Hajjaji and E. Berdimurodov, Ionic liquids as green and smart lubricant application: an overview, *Ionics*, 2022, **28**(11), 4923–4932.

2 S. Akhil, O. J. Curnow, K. J. Walst, R. M. Wang and R. Yunis, Anion effects on thermophysical and thermochemical properties of triaminocyclopropenium-based ionic liquids, *J. Chem. Eng. Data*, 2022, **67**(12), 3602–3615.

3 C. A. Nieto de Castro, S. M. S. Murshed, M. J. V. Lourenço, F. J. V. Santos, M. L. M. Lopes and J. M. P. França, Ionanofluids: New Heat Transfer Fluids for Green Processes Development, in *Green Solvents I*, ed. M. A. Inamuddin, Springer, Dordrecht, the Netherlands, 2012, 233–249.

4 A. Kazakov, J. W. Magee, R. D. Chirico, E. Paulechka, V. Diky, C. D. Muzny, K. Kroenlein and M. Frenkel, *NIST Standard Reference Database 147: Ionic Liquids Database –ILThermo v2.0*, National Institute of Standards and Technology, Gaithersburg, USA, 2017.

5 B. Józwiak, G. Dzido, A. Kolanowska, R. G. Jedrysiak, E. Zorebski, H. F. Greer, M. Dzida and S. Boncel, From lab

and up: superior and economic heat transfer performance of ionanofluids containing long carbon nanotubes and 1-ethyl-3-methylimidazolium thiocyanate, *Int. J. Heat Mass Transfer*, 2021, **172**, 121161.

6   E. A. Chernikova, L. M. Glukhov, V. G. Krasovskiy, L. M. Kustov, M. G. Vorobyeva and A. A. Koroteev, Ionic liquids as heat transfer fluids: comparison with known systems, possible applications, advantages and disadvantages, *Russ. Chem. Rev.*, 2015, **84**(8), 875–890.

7   M. V. Fedoro and A. A. Kornyshev, Ionic liquids at electrified interfaces, *Chem. Rev.*, 2014, **114**(5), 2978–3036.

8   N. V. Plechkova and K. R. Seddon, Applications of ionic liquids in the chemical industry, *Chem. Soc. Rev.*, 2008, **37**, 123–150.

9   G. Chatel, J. F. B. Pereira, V. Debbeti, H. Wang and R. D. Rogers, Mixing ionic liquids-"simple mixtures" or "double salts", *Green Chem.*, 2014, **16**(4), 2051–2083.

10 J. H. Zhang, S. H. Fang, L. Qu, Y. D. Jin, L. Yang and S. Hirano, Synthesis, characterization, and properties of ether-functionalized 1,3-dialkylimidazolium ionic liquids, *Ind. Eng. Chem. Res.*, 2014, **53**(43), 16633–16643.

11 Z. L. Chen, Y. N. Huo, J. Cao, L. Xu and S. G. Zhang, Physicochemical properties of ether-functionalized ionic liquids: understanding their irregular variations with the ether chain length, *Ind. Eng. Chem. Res.*, 2016, **55**(44), 11589–11596.

12 X. X. Ma, F. Li, S. A. Kui, Z. R. Song, L. Gong and D. W. Fang, The static and transport properties of ether-based perrhenate ionic liquids and the ionic parachor application, *J. Chem. Thermodyn.*, 2021, **157**, 106393.

13 H. C. Zhou, L. F. Chen, Z. Wei, Y. J. Lu, C. Peng, B. Zhang, X. J. Zhao, L. Wu and Y. B. Wang, Effect of ionic composition on physicochemical properties of mono-ether functional ionic liquids, *Molecules*, 2019, **24**(17), 3112.

14 R. Leones, R. C. Sabadinic, J. M. S. S. Esperança, A. Pawlicka and M. M. Silva, Effect of storage time on the ionic conductivity of chitosan-solid polymer electrolytes incorporating cyano-based ionic liquids, *Electrochim. Acta*, 2017, **232**(1), 22–29.

15 Y. U. Paulechka, Heat capacity of room-temperature ionic liquids: a critical review, *J. Phys. Chem. Ref. Data*, 2010, **39**(3), 033108.

16 M. Sattari, F. Gharagheizi, P. Ilani-Kashkouli, A. H. Mohammadi and D. Ramjugernath, Estimation of the heat capacity of ionic liquids: a quantitative structure property relationship approach, *Ind. Eng. Chem. Res.*, 2013, **52**(36), 13217–13221.

17 M. Sattari, F. Gharagheizi, P. Ilani-Kashkouli, A. H. Mohammadi and D. Ramjugernath, Development of a group contribution method for the estimation of heat capacities of ionic liquids, *J. Therm. Anal. Calorim.*, 2014, **115**(2), 1863–1882.

18 P. Nancarrow, M. Lewis and L. AbouChacra, Group contribution methods for estimation of ionic liquid heat capacities: critical evaluation and extension, *Chem. Eng. Technol.*, 2015, **38**(4), 632–644.

19 F. Y. Yan, Y. J. Shi, Y. Wang, Q. Z. Jia, Q. Wang and S. Q. Xia, QSPR models for the properties of ionic liquids at variable temperatures based on norm descriptors, *Chem. Eng. Sci.*, 2020, **217**, 115540.

20 A. N. Soriano, A. M. Agapito, L. J. L. I. Lagumbay, A. R. Caparanga and M. H. Li, A simple approach to predict molar heat capacity of ionic liquids using group-additivity method, *J. Taiwan Inst. Chem. Eng.*, 2010, **41**(3), 307–314.

21 A. Rostam, A. Hemmati-Sarapardeh, A. Karkevandi-Talkhooncheh, M. M. Husein, S. Shamshirband and T. Rabczuk, Modeling heat capacity of ionic liquids using group method of data handling: a hybrid and structure-based approach, *Int. J. Heat Mass Transfer*, 2019, **129**, 7–17.

22 A. Barati-Harooni, A. Najafi-Marghmaleki and A. H. Mohammadi, Prediction of heat capacities of ionic liquids using chemical structure based networks, *J. Mol. Liq.*, 2017, **227**, 324–332.

23 X. J. Kang, X. Y. Liu, J. Q. Li, Y. S. Zhao and H. Z. Zhang, Heat capacity prediction of ionic liquids based on quantum chemistry descriptors, *Ind. Eng. Chem. Res.*, 2018, **57**(49), 16989–16994.

24 M. A. A. Rocha, M. Vilas, A. S. M. C. Rodrigues, E. Tojo and L. M. N. B. F. Santos, Physicochemical properties of 2-alkyl-1-ethylpyridinium based ionic liquids, *Fluid Phase Equilib.*, 2016, **428**, 112–120.

25 M. Bendová, Z. Wagner, M. G. Bogdanov, M. Čanji and N. Zdolšek, Heat capacity of 1-hexadecyl-3-methylimidazolium based ionic liquids in solid and liquid phase, *J. Mol. Liq.*, 2020, **305**, 112847.

26 D. H. Zaitsau, A. Schmitz, C. Janiak and S. P. Verevkin, Heat capacities of ionic liquids based on tetrahydrothiophenium cation and NTf$_2$ anion, *Thermochim. Acta*, 2020, **686**, 178547.

27 G. Rai, P. Jain and A. Kumar, Isothermal titration calorimetric study of ionic liquid solutions in alcohols at extreme dilutions: an investigation of ion-solvent interactions, *J. Solution Chem.*, 2016, **45**(9), 1313–1331.

28 E. Paulechka, A. V. Blokhin, A. S. M. C. Rodrigues, M. A. A. Rocha and L. M. N. B. F. Santos, Thermodynamics of long-chain 1-alkyl-3-methylimidazolium bis(trifluoromethanesulfonyl)imide ionic liquids, *J. Chem. Thermodyn.*, 2016, **97**, 331–340.

29 Z. C. Tan, Q. Shi, B. P. Liu and H. T. Zhang, A fully automated adiabatic calorimeter for heat capacity measurement between 80 to 400 K, *J. Therm. Anal. Calorim.*, 2008, **92**, 367–374.

30 D. W. Fang, J. T. Zuo, M. C. Xia, J. Li and J. Z. Yang, Low-temperature heat capacity and standard thermodynamic functions of 1-butyl-3-methylimidazolium lactate, *J. Therm. Anal. Calorim.*, 2018, **133**(2), 1015–1021.

31 D. W. Fang, L. Gong, X. T. Fan, K. H. Liang, X. X. Ma and J. Wei, Low-temperature heat capacity and standard thermodynamic functions of the novel ionic liquid 1-(2-methoxyethyl)-3-ethylImidazolium perrhenate, *J. Therm. Anal. Calorim.*, 2019, **138**, 1437–1442.

32 J. Wei, A. L. Yi, J. L. Miao, J. Liu, D. W. Fang and Z. H. Zhang, Viscosity of binary mixtures of 1-(2-methoxyethyl)-3-

ethylimidazolium thiocyanate ionic liquid with short-chain alcohols, *J. Chem. Thermodyn.*, 2021, **154**, 106320.

33 J. S. Wilkes, J. A. Levisky, R. A. Wilson and C. L. Hussey, Dialkylimidazolium chloroaluminate melts: a new class of room-temperature ionic liquids for electrochemistry, spectroscopy and synthesis, *Inorg. Chem.*, 1982, **21**(3), 1263–1264.

34 J. G. Huddleston, A. E. Visser, W. M. Reichert, H. D. Willauer, G. A. Broker and R. D. Rogers, Characterization and comparison of hydrophilic and hydrophobic room temperature ionic liquids incorporating the imidazolium cation, *Green Chem.*, 2001, **3**(4), 156–164.

35 Z. C. Tan, L. X. Sun, S. H. Meng, L. Li, F. Xu, P. Yu, B. P. Liu and J. B. Zhang, Heat capacities and thermodynamic functions of p-chlorobenzoic acid, *J. Chem. Thermodyn.*, 2002, **34**, 1417.

36 Z. C. Tan, G. Y. Sun, Y. J. Song, L. Wang and D. Z. Nie, An adiabatic calorimeter for heat capacity measurement of small samples-the heat capacity of nonlinear optical materials KTiOPO$_4$ and RbTiOAsO$_4$ Crystals, *Thermochim. Acta*, 2000, **352**, 247–253.

37 D. A. Ditmars, S. Ishihara, S. S. Chang, G. Bernstein and E. D. Wes, Enthalpy and heat-capacity standard reference material: synthetic sapphire (α-Al$_2$O$_3$) from 10 to 2250 K, *J. Res. Natl. Bur. Stand*, 1982, **87**(2), 159.

38 D. G. Archer, Thermodynamic properties of synthetic sapphire (α-Al$_2$O$_3$), Standard peference material 720 and the effect of temperature-scale differences on thermodynamic properties, *J. Phys. Chem. Ref. Data*, 1993, **22**(6), 1441–1453.

39 National Bureau of Standards Certificate, *Standard Reference Material 720*, U. S. Department of Commerce, 1982.

40 R. D. Chirico, M. Frenkel, J. W. Magee, V. Diky, C. D. Muzny, A. F. Kazakov, K. Kroenlein, I. Abdulagatov, G. R. Hardin and W. E. Acree, Improvement of quality in publication of experimental thermophysical property data: challenges, assessment tools, global implementation, and online support, *J. Chem. Eng. Data*, 2013, **58**(10), 2699–2716.

41 L. Zheng, L. Li, Y. F. Guo, W. Guan and D. W. Fang, The isobaric heat capacities and thermodynamic properties of ionic liquid 1-ethylpyridinium bis(trifluoromethylsulfonyl) imide, *J. Therm. Anal. Calorim.*, 2018, **131**, 2943–2949.

42 D. W. Fang, J. T. Zuo, M. C. Xia, J. Tong and J. Li, Low-temperature heat capacities and the thermodynamic functions of ionic liquids 1-heptyl-3-methyl imidazolium perrhenate, *J. Therm. Anal. Calorim.*, 2018, **132**, 2003–2008.

43 B. Tong, Q. S. Liu, Z. C. Tan and W. B. Urs, Thermochemistry of alkyl pyridinium bromide ionic liquids: calorimetric measurements and calculations, *J. Phys. Chem. A*, 2010, **114**, 3782–3787.

© 2024 The Author(s). Published by the Royal Society of Chemistry